JMEPEG (2017) 26:876–884
DOI: 10.1007/s11665-016-2486-5

1059-9495/$19.00

Analytical Modeling of Surface Roughness, Hardness and Residual Stress Induced by Deep Rolling

Frederico C. Magalhães, Alexandre M. Abrão, Berend Denkena, Bernd Breidenstein, and Tobias Mörke

(Submitted April 29, 2016; in revised form November 23, 2016; published online December 21, 2016)

Deep rolling is a mechanical surface treatment that can significantly alter the features of metallic components and despite the fact that it has been used for a long time, to date the influence of the interaction among the principal process parameters has not been thoroughly understood. Aiming to fulfill this gap, this work addresses the effect of deep rolling on surface finish and mechanical properties from the analytical and experimental viewpoints. More specifically, the influence of deep rolling pressure and number of passes on surface roughness, hardness and residual stress induced on AISI 1060 steel is investigated. The findings indicate that the surface roughness after deep rolling is closely related to the yield strength of the work material and the available models can satisfactorily predict the former parameter. Better agreement between the mathematical and experimental hardness values is achieved when a single deep rolling pass is employed, as well as when the yield strength of the work material increases. Compressive residual stress is generally induced after deep rolling, irrespectively of the selected heat treatment and deep rolling parameters. Finally, the model proposed to predict residual stress provides results closest to the experimental data especially when the annealed material is considered.

Keywords deep rolling, hardness, modeling and simulation, residual stress, steel, surface roughness

1. Introduction

Due to the increasing performance required from mechanical components employed in industrial applications, the better understanding of the failure mechanisms of materials is of utmost importance. According to Kukielka (Ref 1), 85% of the failure in mechanical components results from inadequate mechanical properties or surface finish and Collins et al. (Ref 2) report that from 80 to 90% of all macroscopic failures of mechanical components subjected to cyclic loading is due to fatigue.

In general, a superior performance with regard to fatigue life can be expected from components which were previously subjected to processes aimed at improving surface finishing and/or inducing a compressive residual stress (Ref 3), since the possibility of crack nucleation and growth is drastically reduced. Among the available mechanical surface treatment processes employed for these purposes, deep rolling stands out due to the fact that it can increase the fatigue strength of a component from 100 to 240% compared to turning alone (Ref 4). In deep rolling, a ball (or roll) made of a material with high modulus of elasticity is forced against the work material surface, thus promoting an increase in mechanical strength by cold work hardening together with an increase in surface hardness, reduction in surface roughness and the inducement of compressive residual stress up to 100 μm beneath the surface.

Compared to metal cutting operations, analytical modeling of deep rolling has not evolved at the same pace. Bougharriou et al. (Ref 5) report that the greatest advances on the study of deep rolling are concerned with experimental and numerical ap-

Nomenclature

δ	Penetration of rigid ball (μm)
ν_1 and ν_2	Coefficients of Poisson of the deep rolling ball and work materials (−)
E_1 and E_2	Modulus of elasticity of the deep rolling ball and work materials (GPa)
F	Deep rolling force (N)
F_{op}	Optimal deep rolling force (N)
$R_{p0.2}$	Yield strength of the work material (MPa)
R_m	Ultimate tensile strength (MPa)
R_t	Maximum height of the profile after deep rolling (μm)
R_{ti}	Maximum height of the profile before deep rolling (μm)
h	Roughness resulting from the feed rate of the ball (μm)
f	Deep rolling feed rate (mm/rev)
HV_0	Surface hardness values of the work material before deep rolling (kgf/mm^2)
HV_i	Surface hardness values of the work material after deep rolling (kgf/mm^2)
p	Pressure of deep rolling (bar)
z	Number of passes
K	Strength coefficient
n	Strain-hardening exponent
σ_{res}	Residual stress (MPa)

Frederico C. Magalhães, Centro Federal de Educação Tecnológica de Minas Gerais, Av. Amazonas, 7675, Nova Gameleira, Belo Horizonte, MG 30510-000, Brazil; **Alexandre M. Abrão**, Universidade Federal de Minas Gerais, Av. Antônio Carlos, 6627, Pampulha, Belo Horizonte, MG 30270-901, Brazil; and **Berend Denkena, Bernd Breidenstein,** and **Tobias Mörke**, Institute of Production Engineering and Machine Tools, Leibniz Universität Hannover, An der Universität 2, 30823 Garbsen, Germany. Contact e-mail: abrao@ufmg.br.

proaches (the latter with emphasis on finite element methods), especially to assess the intensity and depth of residual stress. Due to the high costs associated with accurate experimental procedures (especially x-ray diffraction) and numerical simulation (time consuming and requiring highly specialized software), the present work aims at proposing an analytical model capable of satisfactorily predicting surface residual stress.

For many decades, Hertz contact theory (Ref 6) has been the only alternative used to represent deep rolling (Ref 7); however, this model neglects the yield strength of the work material. The maximum hardness value recorded after deep rolling is not observed on the surface of the workpiece, but beneath it where the Hertzian stress reaches its highest value. The model proposed by Li et al. (Ref 8) gives satisfactory results for both AA 7075 aluminum alloy and AISI 5140 steel, albeit friction and feed rate of balls/rolls are neglected. Bouzid et al. (Ref 7) presented a model based on Hertz contact theory in which feed rate is taken into account, although surface plastic deformation is not considered. Furthermore, both models (Ref 7, 8) disregard the influence of heat treatment and the effect of number of passes.

A number of studies has been carried out involving experimental and numerical approaches aimed at the better understanding of the nature, intensity and distribution of residual stresses induced by deep rolling (Ref 9, 10). In opposition to experimental and numerical methods, analytical approaches have not received the same degree of attention, especially with regard to the prediction of residual stress (Ref 9, due to the complexity and nonlinear behavior of deep rolling. The above-mentioned models proposed by Bouzid et al. (Ref 7) and Li et al. (Ref 8) are concerned with the prediction of surface roughness only. Therefore, considering the importance of residual stress to the fatigue life of cyclic loaded components and the high cost and specialized work force associated with its both experimental determination and numerical prediction, this work aims to present an analytical model capable of accurately predicting surface roughness, hardness and residual stress induced by deep rolling of AISI 1060 steel subjected to three heat treatment conditions: full and subcritical annealing as well as hardening by quenching and tempering. The predicted values are compared with experimental data and in the case of surface roughness, with the models proposed by Hertz (Ref 6), Bouzid et al. (Ref 7) and Li et al. (Ref 8).

2. Materials and Methods

Bars of AISI 1060 steel were used as work material. The samples were subjected to three heat treatments: full annealing (heating to 975 °C followed by furnace cooling for 70 h) subcritical annealing (heating to 660 °C followed by furnace cooling for 24 h) and hardening (quenching at 830 °C followed by tempering at 440 °C with a soaking time of 1 h). Table 1 summarizes the most relevant mechanical properties (average of four measurements) obtained after each heat treatment.

After turning the samples with coated tungsten carbide inserts ISO grade P15 at a cutting speed of 100 m/min, feed rate of 0.1 mm/rev and maximum depth of cut of 0.15 mm, deep rolling was performed using an Ecoroll HG6-20-5.5 SL20 hydrostatic tool with three tungsten carbide balls (Ø 6.35 mm) equally spaced by 120° around the circumference. This device (shown in Fig. 1 while rolling a tensile test specimen) allows the application of a maximum pressure of 400 bar and operates with a hydraulic fluid possessing a viscosity of 46 mm^2/s at 40 °C. Deep rolling speed and feed were kept constant at 100 m/min and 0.07 mm/rev, respectively. Deep rolling pressure (p) ranged from 50 to 300 bar and either one or three rolling passes (z) were employed.

After deep rolling, the surface roughness (total height of the roughness profile—R_t) of the samples was assessed with a Mahr Perthometer PGK set to a sampling length of 0.80 mm. Surface hardness was measured with a Struers Duramin-5 hardness tester with a load of 500 g applied during 10 s and the near surface residual stress (in the axial direction) was determined applying the $\sin^2 \psi$-method using a GE XRD 3003 TT x-ray diffraction system with a 2 mm diameter collimator, Cr Ka-radiation, and measuring the Fe 211 peak.

3. Results and Discussion

3.1 Surface Roughness

The effect of deep rolling pressure (p) and number of passes (z) on the experimental surface roughness of AISI 1060 steel is shown in Fig. 2, where $z = 0$ represents the surface roughness after turning. For the sake of better observation of the data corresponding to $z = 3$, the axis concerned with number of passes is presented in reverse sequence. In the case of the fully annealed material (Fig. 2a), it can be noted that lowest surface roughness ($R_t \leq 1$ μm) values are obtained applying lower pressure and increased number of passes. This behavior can be explained by the fact that increasing deep rolling pressure causes work material flow, thus impairing surface finish.

As far as the subcritically annealed AISI 1060 steel is concerned, Fig. 2(b) indicates that lower surface roughness values (though within a narrower range) are generated after deep rolling using intermediate pressure and increased number of passes. Although full and subcritical annealing lead to similar hardness values (291 and 295 HV, respectively), the higher yield strength of the latter (402 MPa against 331 MPa) may be the reason why lower R_t values are obtained at higher deep rolling pressures, i.e., when more intense plastic deformation is required and plastic flow does not take place or happens to a lesser extent. Figure 2(c) presents the influence of deep rolling pressure and number of passes on the surface roughness of hardened AISI 1060 steel. In general, considerably lower R_t values are obtained in comparison with the annealed specimens. Furthermore, R_t values below 0.5 μm are generated after deep rolling with minimum number of passes and pressure above 200 bar as a consequence of the high yield strength of this material (1606 MPa).

3.1.1 Analytical Modeling of Surface Roughness. When the Hertz contact pressure theory (Ref 6) is applied to deep rolling, one must bear in mind that this approach resembles an indentation test, i.e., ball feed rate is neglected. In addition to that, the bodies are considered elastic and deformation is purely elastic. The maximum peak to valley height of the profile (R_t) can thus be obtained from the maximum penetration of the rigid ball on the material (δ), see Eq 1:

$$\delta = \lambda \sqrt{\frac{9}{128} A \left(\frac{1 - \nu_1^2}{E_1} + \frac{1 - \nu_2^2}{E_2} \right)^2} F^{2/3} \qquad \text{(Eq 1)}$$

Table 1 Effect of heat treatment on mechanical properties of AISI 1060 steel

	Full annealing	Subcritical annealing	Quenching and tempering
Surface hardness ($HV_{0.5}$)	291	295	756
Yield strength $R_{p0.2}$, MPa	331	402	1606
Ultimate tensile strength R_m, MPa	713	763	2005

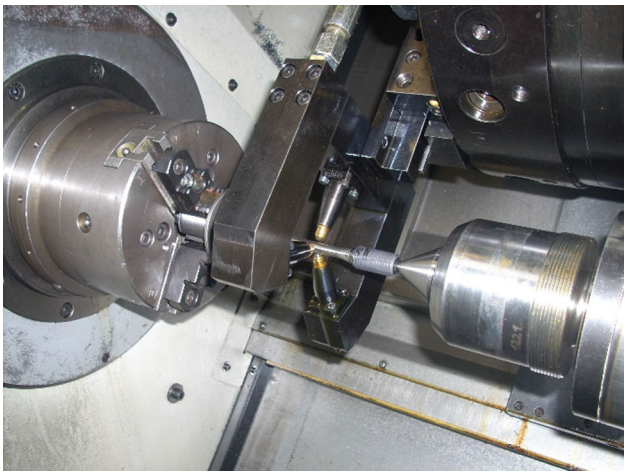

Fig. 1 Deep rolling of a tensile test specimen

$$\theta = \arccos\frac{B}{A} \quad \text{(Eq 2)}$$

The values of A and B can be calculated through Eq 3 and 4, respectively:

$$A = \frac{1}{2}\left(\frac{1}{R_1} + \frac{1}{R_1'} + \frac{1}{R_2} + \frac{1}{R_2'}\right) \quad \text{(Eq 3)}$$

$$B = \frac{1}{2}\sqrt{\left(\frac{1}{R_1} - \frac{1}{R_1'}\right)^2 + \left(\frac{1}{R_2} - \frac{1}{R_2'}\right)^2 + 2\left(\frac{1}{R_1} - \frac{1}{R_1'}\right)\left(\frac{1}{R_2} - \frac{1}{R_2'}\right)\cos 2\beta} \quad \text{(Eq 4)}$$

In order to provide a more realistic model to describe the surface roughness generated by deep rolling, Li et al. (Ref 8) developed an analytical approach based on experimental investigations using AA 7075 aluminum alloy and AISI 5140 steel as work materials. Their model considers the optimal deep

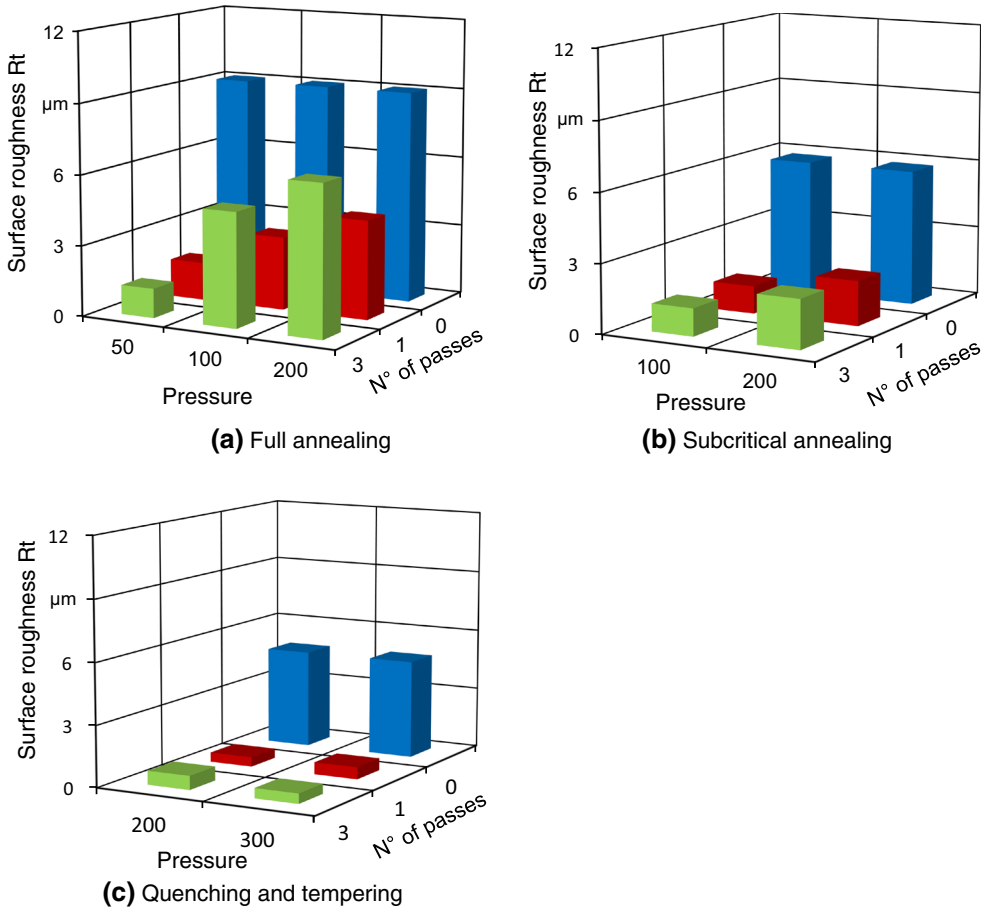

Fig. 2 Effect of deep rolling pressure and number of passes on the surface roughness (R_t) of AISI 1060 steel after three heat treatments: (a) full annealing, (b) subcritical annealing and (c) quenching and tempering (number of passes axis in reverse sequence)

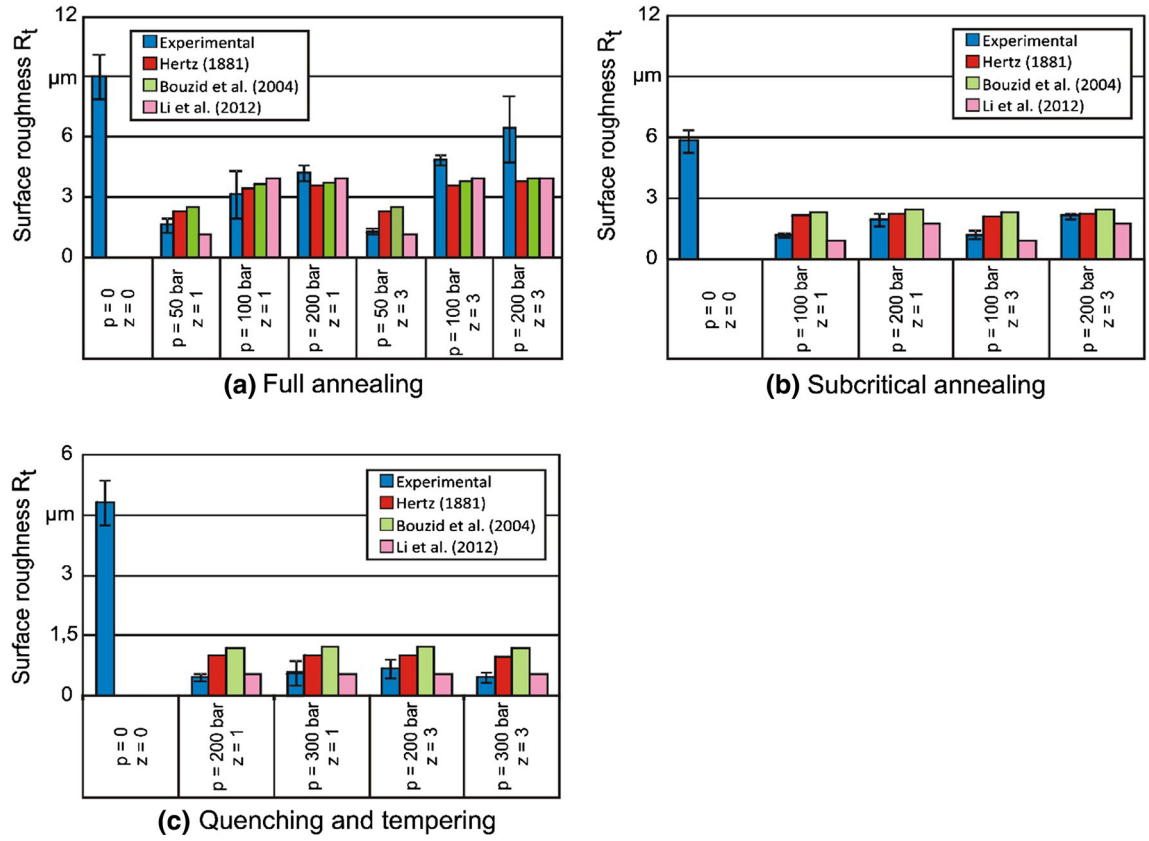

Fig. 3 Experimental and analytical values of R_t before and after deep rolling AISI 1060 steel after three heat treatments: (a) full annealing, (b) subcritical annealing and (c) quenching and tempering

rolling force (F_{op}), as depicted in Eq 5, to determine the penetration of the tool on the work material (δ), see Eq 6:

$$F_{op} = \frac{\pi(1+\varphi)(\cos\alpha - \text{sen}(\alpha-\varphi))R_1R_2R_{p0,2}}{2\cos\alpha}\sqrt{\frac{3R_2}{|R_{1\pm}R_2|}} \quad \text{(Eq 5)}$$

$$\delta = \sqrt[3]{\frac{3(\cos\alpha - \text{sen}(\alpha-\varphi))^2R_{ti}^2|R_{1\pm}R_2|}{8R_1R_2R_{p0,2}^2(1+\varphi)^2\text{sen}^2\alpha}F_{op}^{2/3}}. \quad \text{(Eq 6)}$$

third model proposed by Bouzid et al. (Ref 7) based on (Ref 6) suggests that the feed rate of the deep rolling tool directly affects the workpiece roughness (R_t):

$$R_t = R_{ti} - \delta + h \quad \text{when} \quad \delta \le h \quad \text{(Eq 7)}$$

$$R_t = h \quad \text{when} \quad \delta \ge h \quad \text{(Eq 8)}$$

$$h = \frac{125f^2}{R_1} \quad \text{(Eq 9)}$$

Figure 3 compares the roughness values obtained experimentally (including the corresponding standard deviation) and analytically using the three approaches described above. Due to the fact that the models are not capable of predicting surface roughness after turning, only the experimental data are presented in this case ($p = 0$ and $z = 0$). Figure 3(a) shows the results for fully annealed AISI 1060 steel, where a drastic reduction in surface roughness is obtained after deep rolling. Additionally, lowest roughness is achieved employing a rolling pressure of $p = 50$ bar. As deep rolling pressure is increased, surface roughness is impaired due to plastic flow. Moreover, the number of passes does not seem to affect surface roughness significantly. In contrast, comparing the results provided by the mathematical models with the experimental data, it can be seen that the analytical predictions are closer to the actual R_t values when $z = 1$. The elevation in the number of passes leads to poorer surface finish, which is not detected by the models. For deep rolling with $p = 50$ bar, the model by Li et al. (Ref 8) provides roughness values closest to the experimental data, whereas the three models give similar R_t values as rolling pressure is elevated with a single rolling pass. Though considering plastic deformation only and neglecting elastic recovery, the model by Li et al. (Ref 8) is sensitive to the deep rolling force.

The reason why the models proposed by Hertz (Ref 6) and Bouzid et al. (Ref 7) overestimate roughness resides in the fact that these approaches neglect plastic deformation of the work material. This behavior is highlighted in Fig. 3(b) and (c), concerned with subcritically annealed and hardened AISI 1060 steels, respectively. In spite of the scatter in the experimental data, the three models provide satisfactory estimates of surface roughness after a single rolling pass. Work by Li et al. (Ref 8) reports that when deep rolling materials with low modulus of elasticity, the roughness values calculated using the Hertz model are negative due to the fact that the ball penetration (Eq 1) is higher than the roughness itself, thus limiting its application. Under the same circumstance, the roughness values predicted by the Bouzid model (Eq 3) are constant.

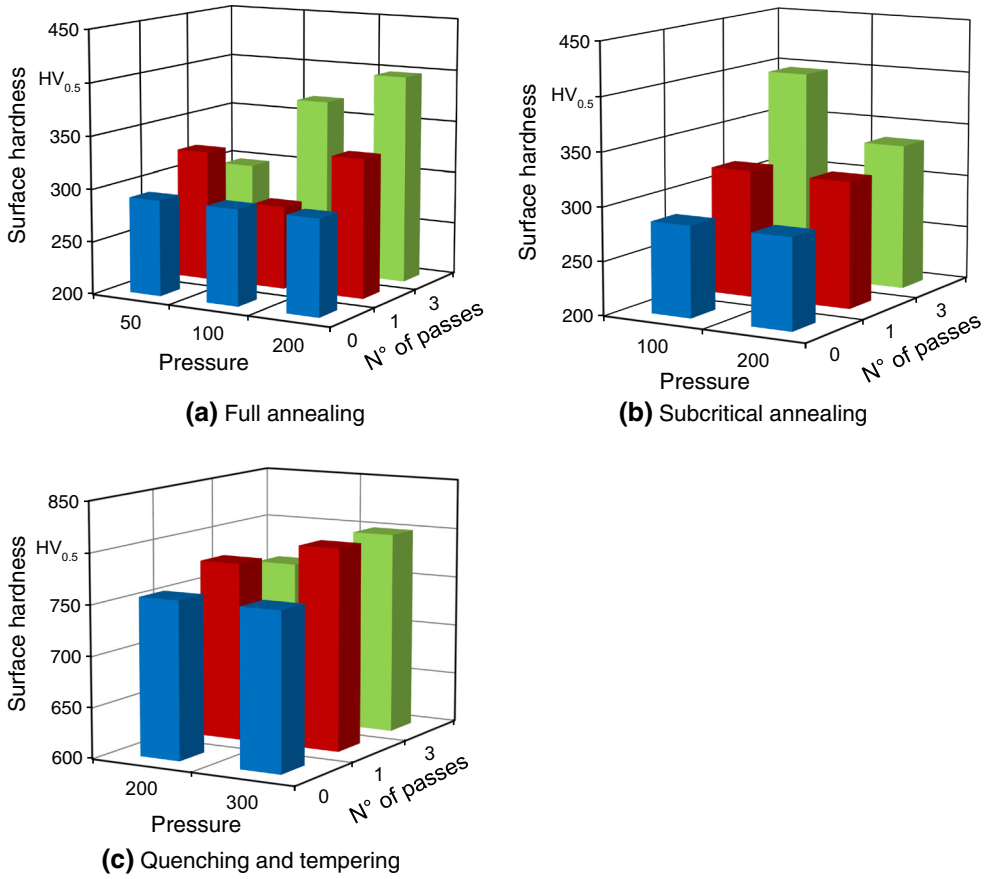

Fig. 4 Effect of deep rolling pressure and number of passes on the surface hardness of AISI 1060 steel after three heat treatments: (a) full annealing, (b) subcritical annealing and (c) quenching and tempering

As the yield strength of the work material is elevated, the difference in surface roughness before and after deep rolling steps up, although the influence of deep rolling pressure is reduced, see Fig. 3(b) and (c). The scatter in the experimental data is diminished as well and, as previously discussed, the model by Li et al. (Ref 8) provides R_t values which are nearer to the experimental values.

3.2 Workpiece Hardness

Figure 4 shows the influence of deep rolling pressure and number of passes on the surface hardness of AISI 1060 steels ($z = 0$ stands for the surface roughness after turning). It can be noticed that each work material responds in a different manner to the elevation of the deep rolling parameters: while surface hardness increases with p and z for the subcritically annealed steel (Fig. 4a) to reach its maximum (400 HV) when $p = 200$ bar and $z = 3$, the highest surface hardness achieved for the fully annealed steel (420 HV) is recorded employing $p = 50$ bar and $z = 3$. In contrast, the surface hardness for the quenched and tempered steel increases with deep rolling pressure but reduces as number of passes is elevated (maximum of 800 HV for $p = 300$ bar and $z = 1$). These findings clearly indicate the importance of the mechanical properties of the work material for the determination of the most suitable deep rolling parameters. As deep rolling pressure and number of passes are elevated, the hardness of the surface layers is expected to increase due to work hardening. The present maps show that with the increase in number of passes, the surface hardness also increases due to condensed grain structure and increased structural homogeneity (Ref 11). Nevertheless, an increase in recovery from work hardening on the surface may take place when a critical deep rolling pressure value above the yield strength of the work material is employed. As a consequence, surface hardness is decreased as shown in Fig. 4(b), (yield strength of 331 MPa for the fully annealed steel against 402 MPa for the subcritically annealed material). A similar behavior is observed for the hardened AISI 1060 steel (Fig. 4c); however, due to its high yield strength (1606 MPa), the critical deep rolling pressure seems to be above $p = 300$ bar.

In order to correlate surface hardness with the deep rolling parameters, a linear regression is proposed. Equation 10 represents the relationship between surface hardness and deep rolling pressure and number of passes for AISI 1060 steel under the three heat treatments considered in this work, i.e., full annealing, subcritical annealing and hardening, respectively:

$$HV_i = 0.9036HV_0 + 0.212p + 15z + 18.6 \quad \text{(Eq 10)}$$

Comparisons between the experimental and empirical values of surface hardness for the three different heat treatments are drawn in Fig. 5. Best agreement for the fully annealed steel is obtained with a deep rolling pressure of $p = 50$ bar (Fig. 5a). Similarly, a satisfactory agreement is obtained for the subcritically annealed steel (Fig. 5b) especially at the lowest deep rolling pressure. Best agreement for the hardened steel (Fig. 5c) is observed after deep rolling with one pass.

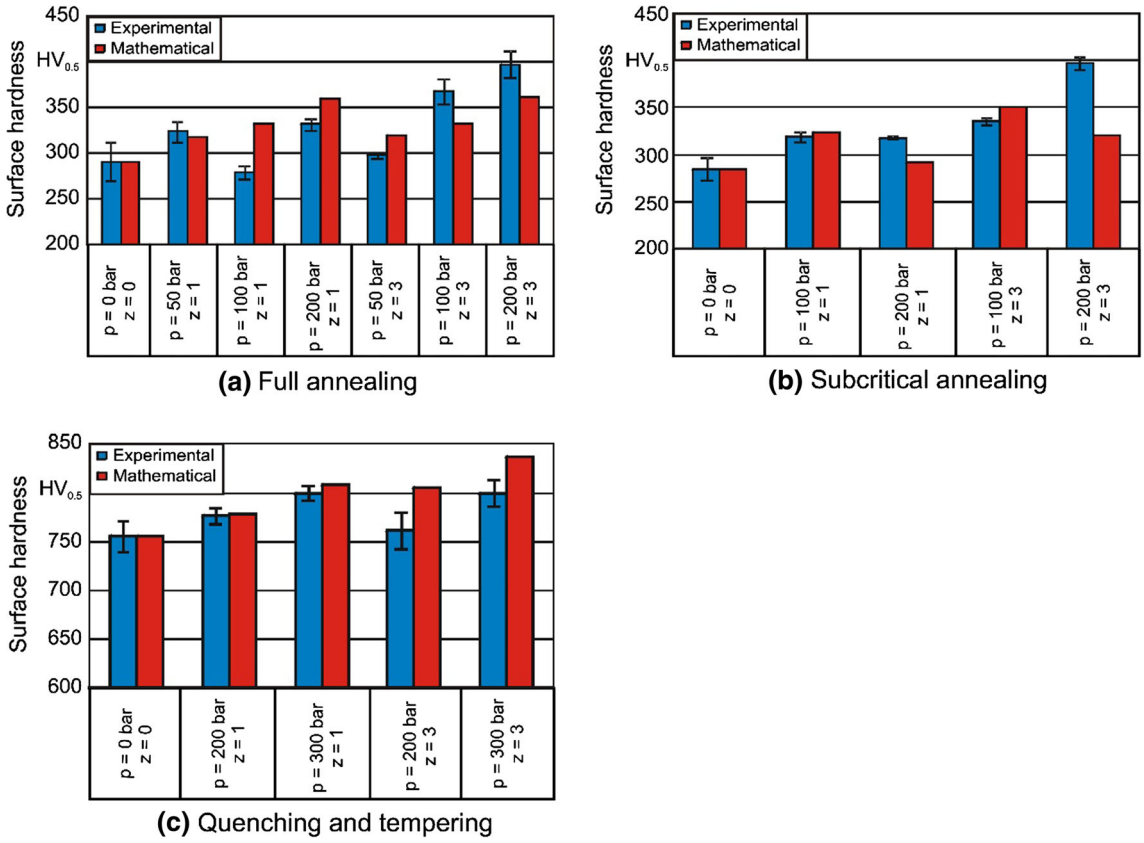

Fig. 5 Experimental and mathematical values of surface hardness before and after deep rolling AISI 1060 steel after three heat treatments: (a) full annealing, (b) subcritical annealing and (c) quenching and tempering

3.3 Residual Stress

Considering that residual stress was measured using the x-ray diffraction method, one must bear in mind that diffraction takes place from a thin surface layer of approximately 20 μm (Ref 12); therefore, near surface stress values are recorded. The influence of deep rolling pressure and number of passes on the near surface residual stress of the fully annealed, subcritically annealed and hardened AISI 1060 steels is given in Fig. 6. Distinct behaviors can be noted when comparing the three heat treatments: in the case of the fully annealed material (Fig. 6a), tensile residual stresses are recorded after turning ($p = 0$ and $z = 0$) to become increasingly compressive after deep rolling and reaching −700 MPa when $p = 100$ bar and $z = 3$. Similarly, tensile residual stresses are recorded after turning the subcritically annealed steel (Fig. 6b); nevertheless, the condition required to achieve compressive residual stresses of highest intensity is $p = 100$ bar and lower number of passes ($z = 2$).

As far as the quenched and tempered material is concerned, a quite distinct trend is observed, see Fig. 6(c). In addition to nearly compressive residual stress after turning, the elevation in deep rolling pressure results in a linear increase in the compressive residual stress, however, number of passes does not possess an influence as markedly as in the case of the annealed samples.

The analytical approach used to model residual stress employs the principal mechanical properties resulting from the different heat treatments applied to AISI 1060 steel. This approach is based on the theories of elasticity and plasticity and considers the reports from Suresh and Giannakopoulos (Ref 13) and Cao et al. (Ref 14), that correlate, respectively, surface hardness with residual stress in the indentation test and surface hardness with yield strength (equivalent stress) for a residual stress free material. Based on the above works, Fig. 7 represents schematically the approach used in order to predict the residual stress induced by turning and deep rolling.

Based on this method, the near surface residual stress (σ_{res}) induced by deep rolling can be calculated through Eq 11:

$$\sigma_{res} = \pm K \cdot \left[\left(\frac{HV_i \cdot R_{p0.2}}{HV_0 \cdot K} \right)^{\frac{1}{n}} - \left(\frac{HV_i \cdot R_{p0.2}}{HV_0 \cdot E} \right) \right]^n \quad \text{(Eq 11)}$$

It can be noticed that Eq 11 depends on the proportionality strength coefficient (K) and the material strain-hardening exponent (n) prior to any mechanical processing. By subjecting distinct metallic materials to tensile testing, Zhongping et al. (Ref 15) successfully managed to correlate K and n with the yield and ultimate tensile strength values of the tested materials.

The reason behind the usage of the yield and ultimate tensile strengths is based on their ratio, employed in the selection of materials (Ref 16). In general, when the ratio between $R_{p0.2}$ and R_m is small, the material is considered as possessing high ability to plastically deform without failure. Therefore, Eq 11 can be rewritten as Eq 12:

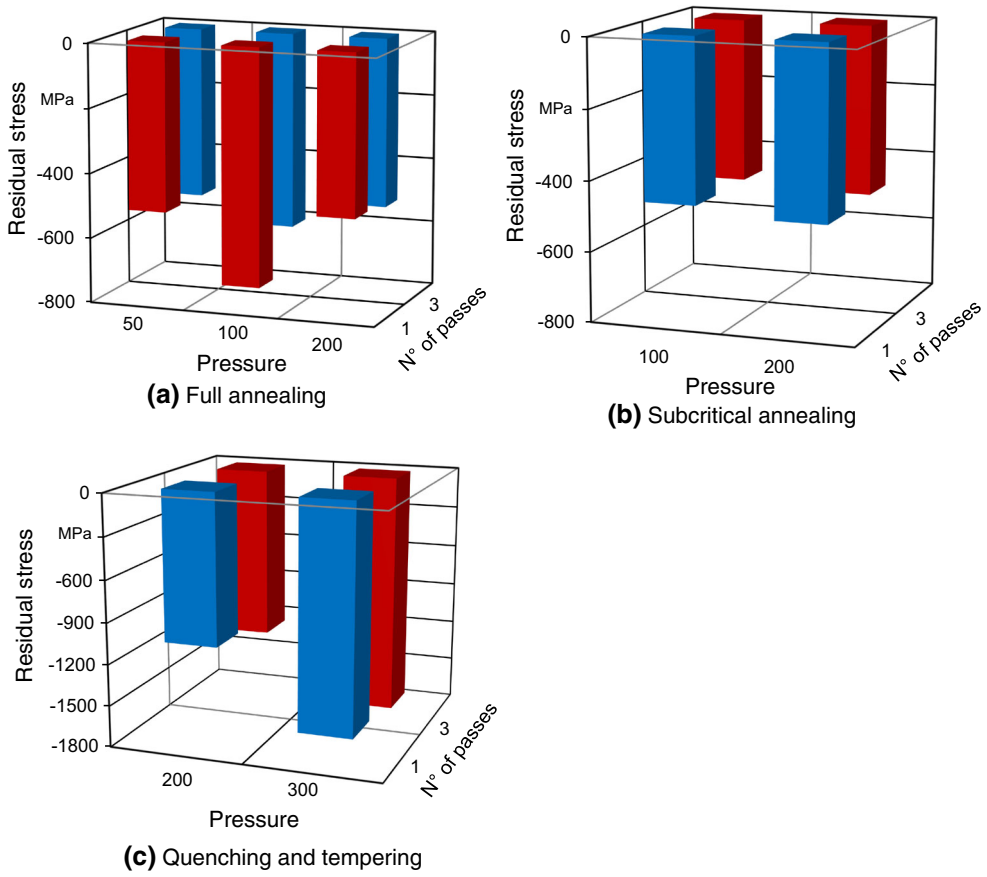

Fig. 6 Effect of deep rolling pressure and number of passes on the residual stress induced on AISI 1060 steel after three heat treatments: (a) full annealing, (b) subcritical annealing and (c) quenching and tempering

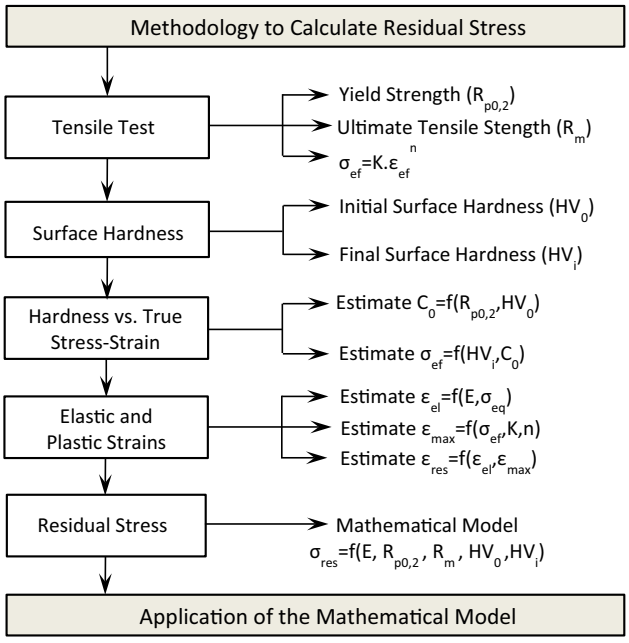

Fig. 7 Mathematical approach used to determine the residual stress after turning and deep rolling

$$\sigma_{\text{res}} = \pm(1 \sim 1.35)\left(\frac{R_{p0.2}^{3/2}}{R_m^{1/2}}\right)\cdot\left(\frac{1}{0.002^C}\right) \cdot\left[\left(\frac{\text{HV}_i\cdot R_{p0.2}}{\text{HV}_0\cdot\left(\frac{R_{p0.2}^{3/2}}{R_m^{1/2}}\right)\cdot(0.002^C)}\right)^{\frac{1}{C}} - \left(\frac{\text{HV}_i\cdot R_{p0.2}}{\text{HV}_0\cdot E}\right)\right]^C \quad \text{(Eq 12)}$$

where

$$C = 0.3\left[1-\left(\frac{R_{p0.2}}{R_m}\right)\right]$$

Although this model has been proposed to predict residual stress after deep rolling, it can be applied to turning owing to the fact that the independent factors (HV_0, HV_i, $R_{p0.2}$ and R_m) were experimentally obtained. Figure 8 presents the influence of deep rolling pressure and number of passes on the residual stresses obtained experimentally and analytically. Irrespectively of the deep rolling parameters and heat treatment employed [full annealing in Fig. 8(a), subcritical annealing in Fig. 8(b) and hardening in Fig. 8(c)], it can be seen that compressive residual stresses are induced by deep rolling.

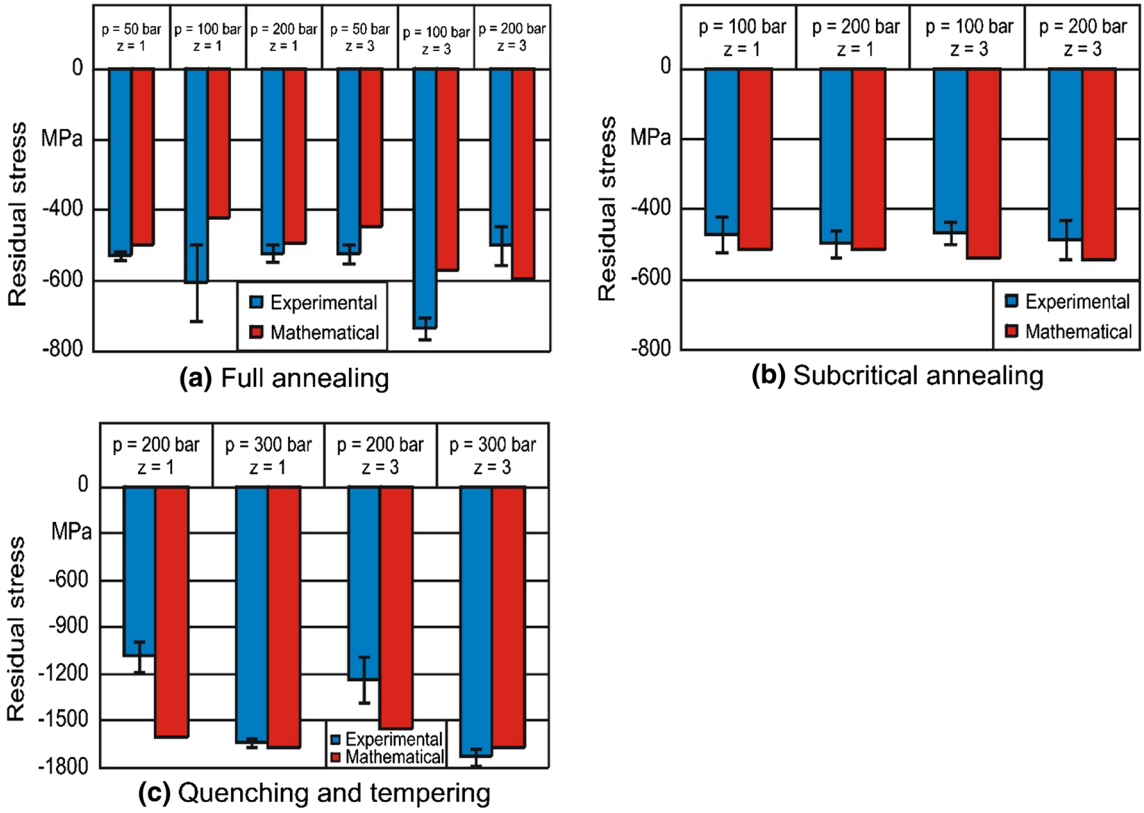

Fig. 8 Experimental and analytical values of residual stress after deep rolling AISI 1060 steel after three heat treatments: (a) full annealing, (b) subcritical annealing and (c) quenching and tempering

Comparing Fig. 8(a) and (c), it can be inferred that additionally to the deep rolling parameters, the induced residual stress is affected by the microstructure/mechanical properties of the work material. For the fully annealed AISI 1060 steel, compressive residual stresses of highest intensity are observed after deep rolling with p = 100 bar, thus suggesting that this value represents the critical deep rolling pressure above which there is no further increase in the magnitude of the residual stress. As a matter of fact, Bernstein and Fuchsbauer (Ref 17) state that deep rolling above the critical pressure value may lead to a decrease in the near surface residual stress [observed in Fig. 8(a) when a deep rolling pressure of 200 bar is applied] or even to its shift to tensile residual stress. In contrast to the appreciable influence of deep rolling pressure and number of passes on the residual stress on the fully annealed steel, the effect of the latter is less pronounced on the subcritically annealed specimens, see Fig. 8(b). Figure 8(c) shows that in the case of the hardened steel, compressive residual stresses of highest intensity are affected markedly by deep rolling pressure and slightly by number of passes, thus suggesting that the critical pressure has yet not been reached. Comparing the experimental and analytical data one can note that, in general, the same trend is observed, exception made for the annealed material rolled at a pressure of 100 bar and the hardened steel rolled at 200 bar. In the case of the fully annealed steel, the largest difference between the average experimental result and the analytical value was 30% (p = 100 bar and z = 1) and the smallest 5% (p = 50 bar and z = 1), whereas for the subcritically annealed material, they were, respectively, 15% (p = 100 bar and z = 3) and 3% (p = 200 bar and z = 1). The hardened steel provided the largest and smallest differences among the tested materials: 47% when p = 200 bar and z = 1 and 2% when p = 300 bar and z = 1. The reason for such divergence may reside on dynamic instabilities during deep rolling; nevertheless, the mathematical model reached a satisfactory result taking into account its simplicity.

4. Conclusion

Surface roughness, hardness and residual stress induced by deep rolling of fully annealed, subcritically annealed and hardened AISI 1060 steel have been analytically modeled and the results compared with experimental data. The following conclusions can be drawn from the present work:

- The lowest surface roughness value attainable after deep rolling is closely related to the yield strength of the work material, i.e., the higher the latter, the higher the value of the deep rolling pressure associated with best surface finish. Moreover, surface roughness decreases with the elevation of the number of deep rolling passes.
- The models proposed by Hertz (Ref 6), Bouzid et al. (Ref 7) and Li et al. (Ref 8) can satisfactorily predict surface roughness after deep rolling, nevertheless the latter produced results closest to the experimental data, especially as the yield strength of the work material is elevated.
- With regard to the surface hardness, the annealed specimens are more affected by the number of passes, while

both deep rolling number of passes and pressure present a marked influence on the hardened steel. In all cases, surface hardness increases with the elevation of the dominant parameter. Better agreement between the mathematical and experimental data is obtained when employing a single deep rolling pass, as well as when the yield strength of the work material increases.

- Compressive residual stresses are induced after deep rolling, irrespectively of the selected heat treatment and deep rolling parameters. Nevertheless, the residual stress induced on the annealed specimens is substantially affected by deep rolling pressure and number of passes, whereas the hardened material is mainly affected by the former.
- The model proposed to predict the residual stress induced by deep rolling provides results closest to the experimental data when the annealed material is considered (lower yield strength). The divergences observed are probably associated with dynamic instabilities (alterations in the regions of contact between ball and work material) and with the nonlinearity associated with deep rolling (changes in the friction coefficient and surface roughness).

Acknowledgments

The authors are indebted to the Brazilian-German Collaborative Research Initiative on Manufacturing Technology (CAPES/DFG BRAGECRIM 029/14), the German Research Foundation for funding the Collaborative Research Centre SFB 653 and CAPES Foundation, Ministry of Education of Brazil, for supporting the post-doctoral work of A.M. Abrão (Grant No. 10118128). Additional thanks go to the Institute of Materials Science of the Leibniz Universität Hannover for the heat treatment and mechanical testing of the specimens, to Ecoroll AG Werkzeugtechnik (Celle, Germany) for the provision of the deep rolling device and to Sandvik Tooling Deutschland GmbH for supplying the cutting tools.

References

1. L. Kukielka, Designating the Field Areas for the Contact of a Rotary Burnishing Element with the Rough Surface of a Part, Providing a High-Quality Product, *J. Mech. Work. Technol.*, 1989, **19**, p 319–356
2. J.A. Collins, H.R. Busby, and G.H. Staab, *Mechanical Design of Machine Elements and Machines: A Failure Prevention Perspective*, 3rd ed., McGraw-Hill Inc, New York City, 2009, p 22–70
3. J. Schijve, *Fatigue of Structures and Materials*, 3rd ed., Kluwer Academic Publishers, Berlin, 1989, p 71–83
4. N.H. Loh, Effects of Ball Burnishing Parameters on Surface Finish—A Literature Survey and Discussion, *Precis. Eng.*, 1988, **10**, p 215–220
5. A. Bougharriou, W. Bouzid, and K. Saï, Analytical Modeling of Surface Profile in Turning and Burnishing, *Int. J. Adv. Manuf. Technol.*, 2014, **75**, p 547–558
6. H. Hertz, Über die Berührung fester elastischer Körper, *Journal für die reine und angewandte Mathematik*, 1881, **92**, p 156–171 (**in German**)
7. W. Bouzid, O. Tsoumarev, and K. Saï, An investigation of surface roughness of burnished AISI, 1042 steel, *Int. J. Adv. Technol.*, 2004, **24**, p 120–125
8. F.L. Li, W. Xia, Z.Y. Zhou, J. Zhao, and Z.Q. Tang, Analytical Prediction and Experimental Verification of Surface Roughness During the Burnishing process, *Int. J. Mach. Tools Manuf*, 2012, **62**, p 67–75
9. A. Rodriguez, L.N.L. Lacalle, A. Celaya, A. Lamikiz, and J. Albizuri, Surface Improvement of Shafts by the Deep Ball-Burnishing Technique, *Surf. Coat. Technol.*, 2012, **206**(11–12), p 2817–2824
10. K. Röttger, *Berichte aus der Produktionstechink—Walzen hartgedrehter oberflächen*, Shaker Verlag, Aachen, 2003 ((in German))
11. G.D. Revankar, R. Shetty, S.R. Roa, and V.N. Gaitonde, Analysis of Surface Roughness and Hardness in Ball Burnishing of Titanium Alloy, *Measurement*, 2014, **58**, p 256–268
12. I.C. Noyan and J.B. Cohen, *Residual Stress—Measurement by Diffraction and Interpretation*, Springer, New York, 1987, p 276
13. A. Suresh and A.E. Giannakopoulos, A New Method for Estimating Residual Stresses by Instrumented Sharp Indentation, *Acta Mater.*, 1998, **45**, p 5755–5767
14. Y. Cao, Z. Xue, X. Chen, and D. Raabe, Correlation Between the Flow Stress and the Nominal Indentation Hardness of Soft Metals, *Scr. Mater.*, 2008, **59**, p 1191–1198
15. Z. Zhongping, C. Donglin, S. Qiang, and Z. Wenzhen, New Formula Relating the Yield-Strain with the Strength Coefficient and the Strain-Hardening Exponent, *J. Mater. Eng. Perform.*, 2004, **13**, p 509–512
16. G.E. Dieter, *Mechanical Metallurgy*, 3rd ed., McGraw-Hill Inc, New York, 1986
17. G. Bernstein and B. Fuchsbauer, Festwalzen und Schwingfestigkeit, *Z. Werkstofftech.*, 1982, **13**, p 103–109 (**in German**)